Controlling Surface Energetics of Silicon by Intermolecular Interactions between Parallel Self-Assembled Molecular Dipoles

ARTICLE *in* THE JOURNAL OF PHYSICAL CHEMISTRY C · JANUARY 2009

Impact Factor: 4.77 · DOI: 10.1021/jp809996b

2 AUTHORS:

Yair Paska

9 PUBLICATIONS **222** CITATIONS

SEE PROFILE

Hossam Haick

Technion - Israel Institute of Technology

158 PUBLICATIONS **4,439** CITATIONS

SEE PROFILE

Controlling Surface Energetics of Silicon by Intermolecular Interactions between Parallel Self-Assembled Molecular Dipoles

Yair Paska and Hossam Haick*

The Department of Chemical Engineering and Russell Barrie Nanotechnology Institute, Technion - Israel Institute of Technology, Haifa 32000, Israel

Received: November 13, 2008; Revised Manuscript Received: November 21, 2008

We show that the electrical properties of Si surfaces can be controlled systematically by the extent of intermolecular interactions between molecular dipoles that self-assemble in parallel on the Si surfaces. We draw this conclusion on the basis of experiments with self-assembled hexyltrichlorosilane molecules on SiO_x/Si surfaces, with different degrees of Si−O−Si intermolecular bonds. Our results indicate that systematic control of intermolecular interactions of organic molecules on a semiconductor surface provides an important additional molecular handle, in addition to varying the individual molecule's dipole, for controlling the surface energetics of semiconductor surfaces and, by extension, of semiconductor- and metal-containing interfaces, thus significantly enhancing the molecular control of electronic surfaces and interfaces.

1. Introduction

The adsorption of polar monolayers on semiconductor surfaces has been studied for a wide range of technological applications, from micro(opto)electronic and nano(opto)electronic devices[1−9] to solar cells[10−12] and (bio)sensors.[3,8,13] Generally, a layer with a net electrical dipole perpendicular to a surface can produce a substantial shift in the surface potential of any material. For a semiconductor or metal, this means a change in the work function, and for a semiconductor, this also means a change in the electron affinity and ionization potential.[3,4,14−19] To a first-order approximation, these changes are due to rigid shifts in the electrostatic potential across the adsorbed molecular layers. This dipole effect is a general one and can be obtained with nonmolecular treatments as well.[20,21] A significant advantage of using molecules, especially organic ones, over nonmolecular treatments is that systematic tuning of the desired permanent molecular dipole moment is possible by a systematic change in the molecules, for example, by appropriate functional group substitutions.[3,4,6,8,22,23]

The interactions of molecular dipoles with the attached substrate were found to be strongly dependent on the intrinsic molecular properties.[1,4,19,24] The total change in the dipole-induced electrostatic potential depends on the molecular dipole[4,6,24,25] as well as the surface coverage[8,22,23,25] of the active molecules and their tilt relative to the surface normal.[4,24] However, little is known about the "lateral" interactions of adjacent molecular dipoles, and even less is known about the correlation between lateral interactions of molecular dipoles and the electrical properties of the structures obtained.

Here, we adapt an approach termed the two-step amine-promoted reaction (TSAPR)[26,27] and investigate the influence of molecular interfacing and interconnecting on the Si surface and interface dipole properties. We do so by forming two major kinds of interactions:[28] a molecule−surface interaction through hydroxyl group and a molecule−molecule interaction between adjacent molecules by Si−O−Si bonds. As we show, the latter interaction can be varied systematically to change the overall dipole moment of the molecular layer concomitantly. These interactions appear to be critical because they lead to significant changes in the overall conduction and/or dipole moment of a self-assembled monolayer of molecules.

2. Experimental Section

2.1. Materials. Silicon(111) n-type (boron, 0.008−0.02 Ω·cm) wafers purchased from Silicon Quest International, Inc. (Santa Clara, CA) were used. All solvents and materials used in the TSAPR process were anhydrous and used as received from Aldrich. Water with a resistivity of >18 MΩ that was obtained from a Barnstead system was used at all times.

2.2. Samples Preparation. The two modes of monolayers were prepared on Si(111) native oxide (2.1 ± 0.2 nm thick) by the TSAPR.[26,27] Before any chemical treatment, each sample was cleaned with H_2O and a flow of N_2, immersed in an 85 °C solution of 4:1:1 v/v/v $H_2O/NH_4OH/H_2O_2$ for 10 min, and rinsed in DI H_2O for 1 min in order to remove inorganic impurities. The samples were then treated via ozone oxidation for 30 min using a UVOCs apparatus, sonicated in chloroform for 5 min, and heated to 300 °C for 30 min. Noncrossed HTS/SiO_x/Si samples were prepared by exposing the clean surface to trimethilamine (TMA) gas for a period of 3 min. The samples were then immersed in 1.5 mM HTS in chloroform solution for 24 h and sonicated for 5 min to remove HTS residues. Crossed HTS/SiO_x/Si samples were made by immersing the noncrossed HTS/SiO_x/Si samples in 90 °C water for 1−24 h, followed by sonication in chloroform for 5 min. All chemical procedures were carried out under ambient conditions (293 K, 40% RH).

2.3. Surface Analysis. The resulting functionalized surfaces were characterized by high-resolution X-ray photoelectron spectroscopy (XPS; Thermo VG Scientific, Sigma Probe, England) using monochromatized Al (Kα) X-rays ($h\nu = 1486.6$ eV) and pass energies ranging from 0 to 1000 eV. Shifts in binding energy were extracted after deconvoluting the raw data, relative to the XPS parameters of the bare samples (e.g., full widths at half-maximum (fwhm), Lorentzian−Gaussian fitting ratio, and SiO_x/Si $2p_{3/2}$ ratio). Time-of-flight secondary ion mass spectroscopy (ToF-SIMS) was carried out using an ION-TOF GmbH instrument. The samples were bombarded over an area

* Corresponding author. E-mail: hhossam@technion.ac.il.

10.1021/jp809996b CCC: $40.75
Published on Web 01/12/2009

SCHEME 1: Simplified scheme for the (a) bare SiO_x/Si, (b) noncrossed HTS/SiO_x/Si. and (c) crossed HTS/SiO_x/Si HTS samples.

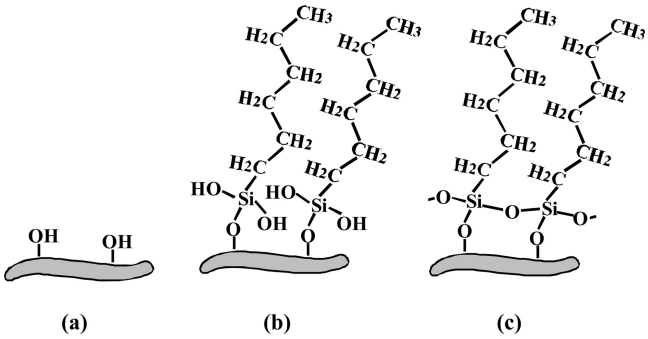

of 100 μm × 100 μm with 50 keV Bi^{5+} ion beams (in addition to 25 keV Bi^+) to increase the intensity of the higher-mass species. The thickness of the HTS self-assembled monolayers (SAMs) was measured by using a spectroscopic phase modulated ellipsometer (M-2000V Automated Angle, J. A. Woollam Co., Inc.) under ambient conditions (293 K, 40% RH). Ellipsometric spectra were recorded over a range of 250−1000 nm at three different angles of incidence: 65°, 70°, and 75°. Four-phase air/SAM/SiO_2/Si substrate model was used to extract the thickness of SAMs layer. An absorption-free Cauchy dispersion of the refractive index with values of n between 1.46 at 1000 nm and 1.61 at 250 nm was assumed for all SAM layers. The measurement was made three times for each sample, and averages were taken.

2.4. Kelvin Probe Measurements. Kelvin probe measurements were carried out under ambient conditions (293 K, 40% RH) with an ambient Kelvin probe package from KP Technology Ltd. (U.K.). This KP package includes a head unit with an integral tip amplifier, a 2 mm tip, a PCI data acquisition system, a digital electronics module, the system software, an optical baseboard with sample and Kelvin probe mounts, a 1 in. manual translator, and a Faraday cage. The work function resolution of the system is 1−3 mV. The Kelvin probe technique measures the contact potential difference (CPD) between a vibrating reference Au probe and the sample. The CPD is defined as the difference in the work function of the two surfaces. Saturating, supra-band-gap illumination was used to neutralize the surface and space charges as much as possible to minimize the bending of the semiconductor bands at the surface. Hence, a CPD measurement under such illumination yields the electron affinity for n-type semiconductors. Subtracting the CPD value under illumination from the dark value gives the band bending at the semiconductor surface. A QTH lamp with a monochromator served as the illumination source. Data was collected for three or more different samples and averaged.

3. Results and Discussion

Si surfaces coated with a 2.1 ± 0.2 nm SiO_x film (hereafter, bare SiO_x/Si) were modified with crossed and noncrossed hexyltrichlorosilane (HTS) self-assembled monolayers (SAMs). (See Scheme 1 for an illustration.) For the sake of convenience, the surface analysis of these samples will be described for the "extreme" cases of HTS/SiO_x/Si samples, with minimal cross-linking (no immersion in 90 °C water) and maximal cross-linking (immersion in 90 °C water for 24 h) unless otherwise stated.[29] To determine the cross-linking differences between both samples, XPS analysis was carried out. Figure 1 presents the Si 2p and C 1s high-resolution XPS spectrum of bare SiO_x/Si

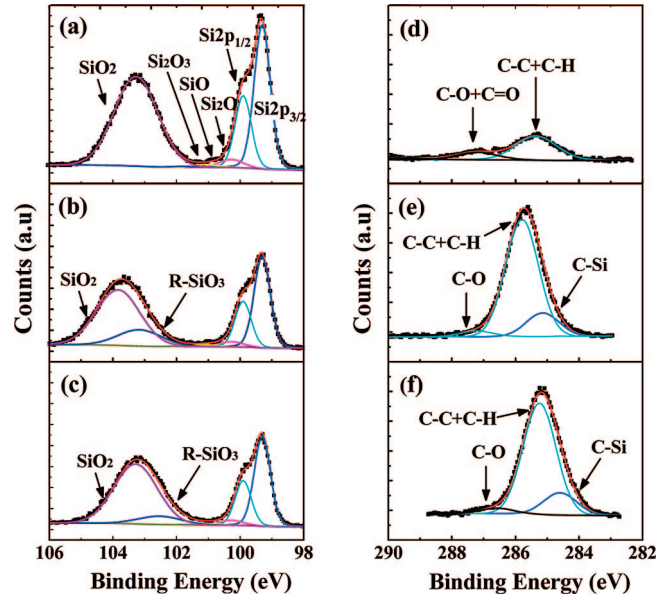

Figure 1. Si 2p XPS data for (a) bare SiO_x/Si, (b) noncrossed HTS/SiO_x/Si, and (c) crossed HTS/SiO_x/Si samples. C 1s XPS data for (d) bare SiO_x/Si, (e) noncrossed HTS/SiO_x/Si, and (f) crossed HTS/SiO_x/Si samples.

and noncrossed and crossed HTS/SiO_x/Si samples. The spectra of bare SiO_x/Si, noncrossed HTS/SiO_x/Si, and crossed HTS/SiO_x/Si samples were shifted by 1.56 ± 0.02, 1.50 ± 0.02, and 2.02 ± 0.02 eV, respectively, for charge correction to the Si $2p_{3/2}$ signal (99.30 ± 0.02 eV). The C 1s peak of the bare sample exhibited three main components corresponding to C−C (285.35 ± 0.02 eV), C−O (287.21 ± 0.02 eV), and C═O (289.44 ± 0.02 eV); see Figure 1d−f. We ascribe the last two peaks to hydrocarbon impurities physically adsorbed to the surface that were impossible to avoid when working under standard laboratory conditions.[30] The C−C peak in the noncrossed samples was shifted by +0.44 ± 0.02 eV and the crossed HTS/SiO_x/Si samples were shifted by −0.12 ± 0.02 eV, relative to the C−C peak of the bare SiO_x/Si. An additional C−Si peak for the noncrossed and crossed HTS/SiO_x/Si samples emerged at −0.65 ± 0.02 eV relative to the binding energy of the C−C bond. Table 1 summarizes the absolute positions of the main C 1s peak and the ratio between the integrated peak areas of the C 1s peak relative to that of Si $2p_{3/2}$ peak, which we denote as C−C/Si and C−Si/Si. As seen in Table 1, the C−C/C−Si ratio for both HTS-coated samples was 5, corresponding to the ratio of C−C and C−Si bonds in the HTS molecules. The C−Si/Si ratios in noncrossed and crossed HTS/SiO_x/Si samples were almost equal, indicating that the coverage of alkyl chains was not affected by the third step of the TSAPR process. This conclusion is supported by ellipsometry measurements that gave a 0.60 ± 0.05 nm HTS thickness in both types of HTS-modified SiO_x/Si samples. For all studied samples, no chlorine signals in the 202 eV region were observed, thus indicating that all of the chlorine groups were replaced by hydroxyl groups.

The Si 2p spectrum of the bare sample exhibited five main peaks. The peaks, as well as the shifts relative to the Si $2p_{3/2}$ (at 99.30 ± 0.02 eV), which we list in parentheses close to the peak name, are as follows:[31] $Si_{1/2}$ (+0.60 ± 0.02 eV), Si_2O (+0.97 ± 0.02 eV), SiO (+1.77 ± 0.02 eV), Si_2O_3 (+2.50 ± 0.02 eV), and SiO_2 (+3.87 ± 0.02 eV). For noncrossed HTS/SiO_x/Si samples, the SiO_2 peaks appeared at +4.54 ± 0.02 eV, and for crossed HTS/SiO_x/Si samples, the SiO_2 peaks appeared at +3.98 ± 0.02 eV relative to the binding energy of Si $2p_{3/2}$

TABLE 1: C 1s XPS Data for the Studied Samples

sample	C−C peak position (eV)[a]	peak shift (eV)[b]	C−C/Si ratio	position of the C−Si peak[a]	peak shift[c]	C−Si/Si ratio
bare SiO_x/Si	285.35 ± 0.02		0.746			
noncrossed HTS/SiO_x/Si	285.79 ± 0.03	+0.44 ± 0.02	4.300	285.15 ± 0.02	−0.65 ± 0.02	0.860
crossed HTS/ SiO_x/Si	285.23 ± 0.02	−0.12 ± 0.02	4.300	284.58 ± 0.02	−0.65± 0.02	0.860

[a] Reported standard deviations are from multiple fits of the raw data for the same sample. [b] Shift relative to the C−C peak. [c] Shift relative to the C−Si peak.

TABLE 2: Si 2p XPS Data for the Studied Samples

sample	position of the R−SiO_3 peak (eV)[a]	peak shift (eV)[b]	R−SiO_3/Si ratio	position of the SiO_2 peak (eV)[a]	peak shift (eV)[c]	SiO_2/Si ratio
bare SiO_x/Si				103.17 ± 0.02		1.584
noncrossed HTS/ SiO_x/Si	103.12 ± 0.02	+0.22 ± 0.02	0.440	103.84 ± 0.02	+0.67 ± 0.02	1.584
crossed HTS/ SiO_x/Si	102.52 ± 0.02	−0.38 ± 0.02	0.243	103.28 ± 0.02	+0.11 ± 0.02	1.712

[a] Reported standard deviations are from multiple fits of the raw data for the same sample. [b] Shift relative to 102.9 eV. [c] Shift relative to the bare SiO_2 peak.

(99.30 ± 0.02 eV). An additional R−SiO_3 peak (where R stands for the C_6 alkyl chain) emerged at +3.82 ± 0.02 eV for the noncrossed HTS/SiO_x/Si samples and at +3.22 ± 0.02 eV for the crossed HTS/SiO_x/Si samples relative to the binding energy of Si $2p_{3/2}$ (99.30 ± 0.02 eV), in good agreement with previous predictions.[32] Table 2 summarizes the absolute and relative values of the different peaks in the Si 2p spectrum of the studied samples.

Generally speaking, the formation of cross-links between trichlorosilane molecules on SiO_x/Si is expressed by an increase in the SiO_2 peak intensity and a decrease in the R−SiO_3 peak intensity. Furthermore, upon the formation of cross-links, the Si 2p peak moves to higher energies and adds to the SiO_2 peak and vice versa. With this in mind, our results have shown that the SiO_2/Si $2p_{3/2}$ ratios in the bare and noncrossed HTS/SiO_x/Si samples were almost equal. In contrast, the SiO_2/Si $2p_{3/2}$ ratio in the crossed HTS/SiO_x/Si sample was ca. 8 ± 1% higher than that of bare SiO_x/Si. This change can be understood as the formation of an extra submonolayer of silicon oxide. Comparing the R−SiO_3/Si $2p_{3/2}$ ratios for both crossed and noncrossed samples showed that 55 ± 2% of the HTS molecules were cross-linked in the third step of the TSAPR process.

On the basis of the XPS results, we conclude that the third step of the TSAPR process affects only the cross-linking between the HTS molecules (Table 2) but not the coverage of the alkyl chains on the surface (Table 1). To determine the real (or absolute) number of cross-linked molecules in HTS/SiO_x/Si samples (rather than relative values, as extracted from the XPS results), we analyzed the samples by means of time-of-flight secondary ion mass spectroscopy (ToF SIMS). Figure 2 presents selected ToF SIMS negative spectrum peaks of all studied samples, normalized over the total number of counts. A combination of a wide variety of ion species, especially $C_6H_{13}SiO_2H$ ($RSiO_2$) at $m/z = 145$ and a series of dimers such as $(C_6H_{13})_2Si_2(OH)_2O_3H_3$ ($R_2Si_2O_5$) at $m/z = 311$, allowed us to determine the (absolute) number of cross-linked molecules in both HTS-modified samples.[33] The ratio between the R−SiO_2 peaks of crossed HTS/SiO_x/Si samples to that of noncrossed HTS/SiO_x/Si samples was 0.53 ± 0.04. This value is in very good agreement with the 0.55 ± 0.02 value obtained by XPS. The intensity of the R_2−Si_2O_5 peaks in the noncrossed HTS/SiO_x/Si sample was within the background noise, whereas the intensity for the crossed HTS/SiO_x/Si sample was significant, indicating the absence (or very minor extent) of cross-linking in the noncrossed HTS/SiO_x/Si sample. In view of these findings, the adsorption of HTS molecules on SiO_x/Si substrates through uncontrolled silanization (adsorption of HTS without pretreating the surfaces with TMA) formed ca. 25 ± 5% cross-links (not shown). Previous studies have shown that a variable number of water molecules during the preparation process is a major factor in deviations in the extent of cross-linking when an uncontrolled silanization process is used.[34]

The effects of HTS cross-linking on the electrical properties of the free surface were evaluated by measuring the surface potential using the Kelvin probe. The work function, relative to that of the Au reference, was measured to be −0.30 ± 0.02 eV for the bare SiO_x/Si, −0.58 ± 0.03 eV for the noncrossed HTS/SiO_x/Si, and −0.46 ± 0.02 eV for the crossed HTS/SiO_x/Si sample. Considering these results from another perspective, the HTS monolayer in the crossed and noncrossed HTS/SiO_x/Si samples changed the work function of the SiO_x/Si substrate by −0.16 ± 0.02 and −0.28 ± 0.02 eV, respectively. For dipoles on a semiconductor surface, the work function will vary with the potential drop, $\Delta\Phi$, over a surface dipole layer, which is a function of the dipole moment, μ, according to[35]

$$\Delta\Phi = \frac{N\mu \cos\theta}{\varepsilon\varepsilon_o} \quad (1)$$

Here, N is the density of the dipoles. In the case of molecules, θ is the average tilt of the molecules relative to the surface normal ε is the effective dielectric constant of the molecular film (including any depolarization effects[8]), and ε_o is the permittivity of free space. The energies of the band at the semiconductor surface are normally shifted, compared to their value in the bulk, because of surface charges and the molecule−surface interaction. This difference is the band bending (BB), which is taken to be positive for an n-type semiconductor with a depletion layer.

As discussed earlier, the coverage and tilt angle of the noncrossed and crossed HTS molecules on SiO_x/Si surfaces are equal. The BB was measured (Experimental Section) and found to be constant (80 ± 5 meV) in all studied samples. Assuming that the dielectric constant of the HTS molecules in both HTS-modified samples are equal, the work function change in these samples can originate only from dipole moment effects (eq 1). Dividing $\Delta\Phi$ in the crossed HTS/SiO_x/Si (−0.16 ± 0.02 eV) by that in the noncrossed HTS/SiO_x/Si (−0.28 ± 0.02 eV) yields a value of 0.57 ± 0.07 (Figure 3, black, filled circles; left y axis). The obtained value is similar, within experimental error, to the R−SiO_3 ratio (0.55 ± 0.02) extracted by XPS. These

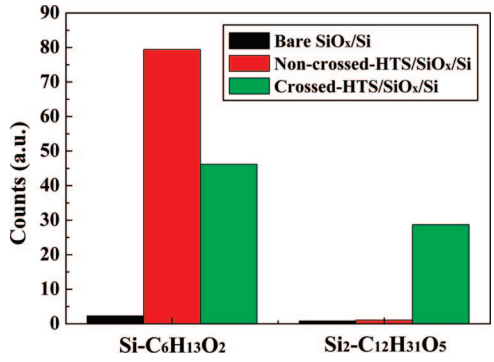

Figure 2. Selected ToF SIMS negative spectrum peaks of bare SiO_x/Si and noncrossed and crossed HTS/SiO_x/Si samples, normalized over the total number of counts. The combination of $C_6H_{13}SiO_2H$ (RiO_2) at $m/z = 145$ and a series of dimers such as $(C_6H_{13})_2Si_2(OH)_2O_3H_3$ ($R_2Si_2O_5$) at $m/z = 311$ determine the (absolute) number of cross-linked molecules in both HTS-modified samples.

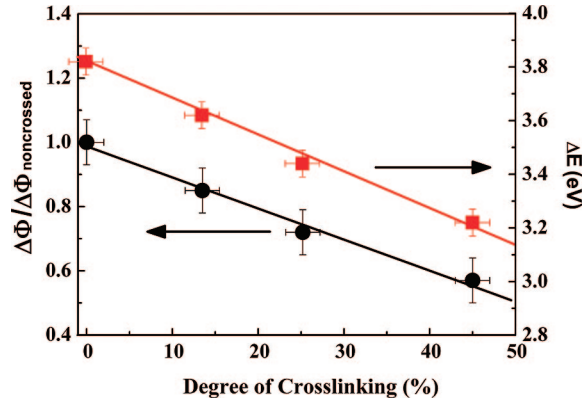

Figure 3. $\Delta\Phi/\Delta\Phi_{noncrossed}$ ratio (black, filled circles; left y axis) determined by the Kelvin probe and shifts of R−SiO_3 XPS relative to the Si $2p_{3/2}$ peak (ΔE; red, filled squares; right y axis) vs the degree of cross-linking between the HTS molecules on SiO_x/Si surfaces (x axis).

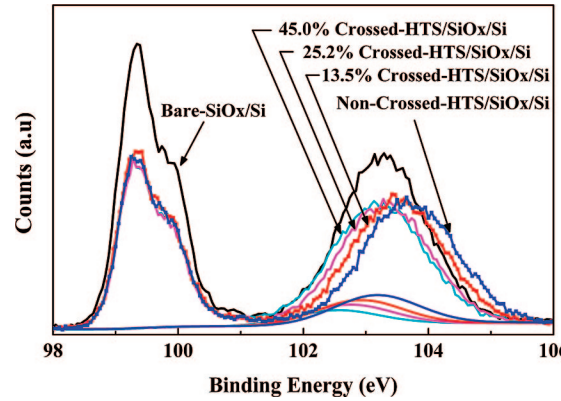

Figure 4. Raw Si 2p XPS data and the R−SiO_3 fitted peak for bare SiO_x/Si surfaces, noncrossed HTS/SiO_x/Si, and 13.5-, 25.2-, and 45.0%-crossed HTS/SiO_x/Si samples. Shifts in binding energy were extracted after deconvoluting the raw data relative to the XPS parameters of the bare samples (fwhm, Lorentzian−Gaussian fitting ratio, and SiO_x/Si $2p_{3/2}$ ratio).

results suggest that the dipole moment of the functionalized surface correlates with the extent of cross-linking of the HTS molecule on the SiO_x/Si surface.

With this in mind, the degree of cross-linking was varied experimentally to reach values lower than those mentioned in the previous sections. This was achieved by immersing the noncrossed HTS/SiO_x/Si sample for 5.5 and 11 h in water at 90 °C. XPS analysis of these samples revealed 13.5% and 25.2% cross-linking of the HTS molecules after immersing the noncrossed HTS/SiO_x/Si sample for 5.5 and 11 h, respectively. As seen in Figure 3 (black, filled circles; left y axis), a linear correlation was found between the extent of cross-linking, expressed by the R−SiO_3 integrated area ratio, and the change in the work function of the SiO_x/Si sample. In other words, by varying the number of Si−O−Si interconnecting bonds between the HTS molecules, we were able to change the work function of the SiO_x/Si surface without affecting the coverage or the tilt of the angle of the molecules.

From eq 1, we learn that the negative values of $\Delta\Phi$ indicate positive dipole moment of the HTS molecules in both noncrossed and crossed HTS/SiO_x/Si samples. Note that the positive dipole moment is defined as having a negative pole directed out of the surface.[4,24] In this case, charges transfer from Si (electronegativity, χ, of 1.90) to the molecule's carbon ($\chi = 2.55$) atom that is located close to the SiOx surface and increase the effective dipole moment of the HTS SAM. The introduction of intermolecular Si−O−Si bonds between the adjacent HTS molecules redistributes the charge in the sublayer of silicon oxide (that results from the intermolecular bonding) and decreases the dipole moment further, compared to that of noncrossed HTS/SiO_x/Si samples. The electronegativity value of oxygen ($\chi = 3.44$) atoms, which is higher than for both Si ($\chi = 1.90$) and carbon ($\chi = 2.55$) atoms, supports this explanation. On the basis of complementary results, the adsorption of HTS molecules on SiO_x/Si substrates through uncontrolled silanization (i.e., adsorption of HTS without pretreating the surfaces with TMA) formed ca. 25 ± 5% cross-links. For this sample, the obtained $\Delta\Phi/\Delta\Phi$ noncrossed ratio and shifts of R−SiO_3 XPS relative to the Si $2p_{3/2}$ peak (ΔE) were similar to those presented in Figure 3 for structures with ~25% cross-linking (within experimental error).

Supporting evidence for the same cross-linking-induced dipolar effect can be found in the XPS R−SiO_3 peak shift relative to the binding energy of Si $2p_{3/2}$ as a function of the extent of cross-linking (Figure 3, right y axis, and Figure 4). A chemical shift of the SiO_2 XPS peak has been reported to increase as a function of the silicon oxide thickness.[36] This increase was explained to be a result of a combination of the following effects: (i) initial state effects,[37] which refer to structural and compositional features of the material that influence the energy level of the core state prior to interaction with the exciting photon; (ii) final state effects,[38,39] which refer to mechanisms that serve to stabilize or destabilize the positively charged core−hole state that is formed upon ejection of the photoelectron from the emitting atom; and/or (iii) extrinsic effects,[39] which are related to details of the experimental conditions. For our samples, extrinsic effects were corrected by charge correction to the Si $2p_{3/2}$ signal (99.30 ± 0.02 eV). Final state effects are related to the distance change of the emitters (Si atoms) contributing to the spectrum from the silicon substrate.[39] However, in our case the silicon oxide thickness is constant for all HTS/SiO_x/Si samples. Having eliminated extrinsic effects and final state effects from consideration, we believe that the XPS shifts originate from initial state effects—the cross-linking. Grunthaner et al.[37] related the peak shifts to the changes in Si−O−Si bond angle as the eight-membered ring of Si_4O_4 is formed, on which the charge transfer from silicon to oxygen depends. This interpretation is a well-supplemented view of the systematic redistribution of charge and the effective dipole moment changes.

4. Summary and Conclusions

Our results provide experimental evidence that systematic control of the work function of SiO_x/Si can be achieved not only by controlling the properties of the molecular dipoles but also by the intermolecular interactions between them. The only condition to be fulfilled is that, on average, the adsorbed molecules will have a dipole moment perpendicular to the surface. This is attributed to the fact that the intermolecular bonds between parallel molecular dipoles change the overall dipole moment of the organic layer. The first major implication of this work is that the systematic control of semiconductor surface energetics or the semiconductor-containing interface, by means of organic molecules, is also possible via a unique synthesis route without the need to change the individual molecule's dipole. The second major implication is that one can change the molecular controllability over a given (unique) electronic device without the need to replace the adsorbed molecules physically on the surface by hard synthesis and/or subsequent functionalizations.

Acknowledgment. We acknowledge the Marie Curie Excellance Grant of the FP6, the US-Israel Binational Science Foundation, and the Russell Berrie Nanotechnology Institute for financial support, Prof. David Cahen (Weizmann Institute of Science) for fruitful comments on the ms, and Mr. Eladd Har-Even (Technion-IIT) for experimental assistance. H.H. holds the Horev Chair for the Leaders in Science and Technology.

References and Notes

(1) Ishii, H.; Sugiyama, K.; Ito, E.; Seki, K. *Adv. Mater.* **1999**, *11*, 605–625.

(2) Chabinyc, M. L.; Chen, X.; Holmlin, R. E.; Jacobs, H.; Skulason, H.; Frisbie, C. D.; Mujica, V.; Ratner, M. A.; Rampi, M. A.; Whitesides, G. M. *J. Am. Chem. Soc.* **2002**, *124*, 11730–11736.

(3) Ashkenasy, G.; Cahen, D.; Cohen, R.; Shanzer, A.; Vilan, A. *Acc. Chem. Res.* **2002**, *35*, 121–128.

(4) Vilan, A.; Cahen, D. *Trends Biotechnol.* **2002**, *20*, 22–29.

(5) Frolov, L.; Rosenwaks, Y.; Carmeli, C.; Carmeli, I. *Adv. Mater.* **2005**, *17*, 2434–2437.

(6) de Boer, B.; Hadipour, A.; Mandoc, M. M.; Van Woudenbergh, T.; Blom, P. W. M. *Adv. Mater.* **2005**, *17*, 621–625.

(7) Haick, H.; Ambrico, M.; Ligonzo, T.; Tung, R. T.; Cahen, D. *J. Am. Chem. Soc.* **2006**, *128*, 6854–6869.

(8) Natan, A.; Kronik, L.; Haick, H.; Tung, R. T. *Adv. Mater.* **2007**, *19*, 4103–4117.

(9) Marmont, P.; Battaglini, N.; Lang, P.; Horowitz, G.; Hwang, J.; Kahn, A.; Amato, C.; Calas, P. *Org. Electron.* **2008**, *9*, 419–424.

(10) Rühle, S.; Greenshtein, M.; Chen., S.-G.; Merson, A; Pizem, H.; Sukenik, C. S.; Cahen, D.; Zaban, A. *J. Phys. Chem. B* **2005**, *109*, 18907–18913.

(11) Zhao, W.; Salomon, E.; Zhang, Q.; Barlow, S.; Marder, S.; Kahn, A. *Phys. Rev. B* **2008**, *77*, 165336/1–165336/6.

(12) Olson, D. C.; Lee, Y.-J.; White, M. S.; Kopidakis, N.; Shaheen, S. E.; Ginley, D. S.; Voigt, J. A.; Hsu, J. W. P. *J. Phys. Chem. C* **2008**, *112*, 9544–9547.

(13) Cahen, D.; Naaman, R.; Vager, Z. *Adv. Funct. Mater.* **2005**, *15*, 1571–1578.

(14) Taylor, D. M.; Bayes, G. F. *Phys. Rev. E* **1994**, *49*, 1439–1449.

(15) Nuesch, F.; Rotzinger, F.; Si-Ahmed, L.; Zuppiroli, L. *Chem. Phys. Lett.* **1998**, *288*, 861–867.

(16) Kruger, J.; Bach, U.; Gratzel, M. *Adv. Mater.* **2000**, *12*, 447–451.

(17) Ganzorig, C.; Kwak, K.-J.; Yagi, K.; Fujihira, M. *Appl. Phys. Lett.* **2001**, *79*, 272–274.

(18) Salomon, A.; Berkovich, D.; Cahen, D. *Appl. Phys. Lett.* **2003**, *82*, 1051–1053.

(19) Magid, I.; Burstein, L.; Seitz, O.; Segev, L.; Kronik, L.; Rosenwaks, Y. *J. Phys. Chem. C* **2008**, *112*, 7145–7150.

(20) Franciosi, A.; Van de Walle, C. G. *Surf. Sci. Rep.* **1996**, *25*, 1–40.

(21) Tung, R. T. *Mater. Sci. Eng., R: Reports* **2001**, *R35*, 1–138.

(22) Gozlan, N.; Tisch, U.; Haick, H. *J. Phys. Chem. C* **2008**, *112*, 12988–12992.

(23) Gozlan, N.; Haick, H. *J. Phys. Chem. C* **2008**, *112*, 12599–12601.

(24) Ashkenasy, G.; Cahen, D.; Cohen, R.; Shanzer, A.; Vilan, A. *Acc. Chem. Res.* **2002**, *35*, 121–128.

(25) Bruening, M.; Cohen, R.; Guillemoles, J. F.; Moav, T.; Libman, J.; Shanzer, A.; Cahen, D. *J. Am. Chem. Soc.* **1997**, *119*, 5720–5728.

(26) Hair, M. L.; Tripp, C. P. *Colloids Surf., A* **1995**, *105*, 95–103.

(27) Tripp, C. P.; Hair, M. L. *J. Phys. Chem.* **1993**, *97*, 5693–5698.

(28) Tripp, C. P.; Hair, M. L. *Langmuir* **1995**, *11*, 149–155.

(29) The surface analysis of HTS/SiO_x/Si samples having "intermediate" degrees of cross-linking was characterized in a similar manner to the two extreme cross-linking cases.

(30) The amount of hydrocarbon impurities was observed equally for all samples. This indicates that the obtained differences between the samples are not from the additional (contamination) adlayer but rather are from the monolayer per se.

(31) Himpsel, F. J.; McFeely, F. R.; Taleb-Ibrahimi, A.; Yarmoff, J. A.; Hollinger, G. *Phys. Rev. B* **1988**, *38*, 6084–6096.

(32) Alexander, M. R.; Short, R. D.; Jones, F. R.; Michaeli, W.; Blomfield, C. J. *Appl. Surf. Sci.* **1999**, *137*, 179–183.

(33) Houssiau, L.; Bertrand, P. *Appl. Surf. Sci.* **2003**, *203−204*, 580–585.

(34) Tripp, C. P.; Hair, M. L. *Langmuir* **1992**, *8*, 1120–1126.

(35) Moench, W. *Semiconductor Surfaces and Interfaces*; Springer-Verlag: Berlin, Germany, 2001.

(36) Ulgut, B.; Suzer, S. *J. Phys. Chem. B* **2003**, *107*, 2939–2943.

(37) Grunthaner, F. J.; Grunthaner, P. J.; Vasquez, R. P.; Lewis, B. F.; Maserjian, J.; Madhukar, A. *Phys. Rev. Lett.* **1979**, 1683–1686.

(38) Kobayashi, H.; Kubota, T.; Kawa, H.; Nakato, Y.; Nishiyama, M. *Appl. Phys. Lett.* **1998**, *73*, 933–935.

(39) Zhang, K. Z.; Greeley, J. N.; Holl, M. M. B.; McFeely, F. R. *J. Appl. Phys.* **1997**, *82*, 2298–2307.

JP809996B